Full-factorial design and mathematical models of fixed-bed column adsorption of hexavalent chromium by S. glauca

Alka Banchhor
Bhilai Institute of Technology, Durg, India
Madhurima Pandey (pandeymadhurima01@gmail.com)
Bhilai Institute of Technology, Durg, India
Piyush Kant Pandey
Bhilai Institute of Technology, Durg, India

Research Article

Keywords: Cr(VI), Full factorial design, column adsorption, Thomas model, Yoon-Nelson model, Adam's-Bohart model

Posted Date: April 3rd, 2023

DOI: https://doi.org/10.21203/rs.3.rs-2760235/v1

Abstract

The effective removal of hexavalent chromium is a very important issue for many countries. There is rising interest in the use of inexpensive and widely accessible materials for the adsorption of Cr (VI). *Simarouba glauca*, a easily available medicinal plant was found to be very effective in removing Cr(VI) from aqueous medium. First part of the study deals with the implementation of 2^5 Full factorial design technique to investigate adsorption of Cr(VI) onto *S. glauca*. It aided in the assessment of the main effects and interactions between the dose of *S. glauca*, pH, temperature, initial Cr(VI) concentration, and time. The adsorption significance was predicted through ANOVA, T-Test, Pareto chart, main effect and interaction plot. The second part of the study deals with the investigating potential of *S. glauca* by continuous adsorption mode in a fixed-bed column. The effects of Cr(VI) inlet concentration (50,100,150 mg/L), flow rate (13 and 21 mL/min) an *S. glauca* bed height (30, 36, 40 and 45 cm) on the breakthrough characteristics of the adsorption system were determined. The highest bed capacity of 611.69 mg/g was obtained using 100 mg/L inlet Cr(VI) concentration, 45 cm bed height and 13 mL/min flow rate. Three well-known fixed-bed adsorption models, the Thomas, Yoon-Nelson models and Adam's-Bohart were used to match the adsorption data. With correlation coefficients of 0.99 under various circumstances, the results suit the Thomas and Yoon-Nelson models well. According to this study, we may utilise this method to remediate chromium-contaminated water in industrial settings.

Introduction

Chromium, a typical contaminant is discharged as process waste streams into natural water from various industries such as tanneries, electronic device manufacturing units, power-generation, mining and metal-plating facilities. Chromium concentrations in this waste streams are higher than allowed by law. The World Health Organization's drinking water recommendations state that the maximum permitted level for hexavalent chromium Cr(VI) is 0.05 mg/L (WHO 2020). As well as being highly poisonous, Cr(VI) is transportable in the environment. As a possible cause of several cancer diseases, Cr(VI) can quickly pass through the cell wall and exert its harmful influence within the cell. Long-term and short-term exposure levels above the MCL can harm the liver, kidney circulation, nerve tissue, skin and stomach ulceration and dermatitis (Sharma et al. 2022). So developing a removal technique becomes mandatory before releasing Cr(VI) contaminated wastes into various environmental matrices.

Adsorption processes using natural adsorbent or agricultural waste products have become a more advantageous alternative for wastewater treatment. The use of biosorbent for chromium adsorption offers a number of significant benefits, including the ability to reduce the concentration of chromium ions to an extremely low level and the low cost of the adsorbent material itself. For the removal of Cr(VI), a variety of activated carbons, industrial wastes, agricultural wastes, and non-living and living biosorbents are frequently used (Bayuo 2021). Among various biosorbent appropriate for the removal of Cr(VI), *Simarouba glauca* (*S. glauca*), a plant biosorbent appeared to be a highly efficient in eliminating Cr(VI) from aqueous solution when performed in batch adsorption mode. The reported adsorption capacity in batch adsorption mode was 10.9 mg/g (Banchhor et al. 2021).

Throughout the adsorption process, various aspects are involved. It becomes important to analyze the influence of all those aspects upon the response of the process and also to achieve the best overall optimization of the system. The typical "one variable at a time" approach adopted by researchers in the past implicitly presupposes that all the variables are independent. Usually, this is not the case, and in these circumstances, it is important to take various aspects into account at once. For this purpose, 2^k full-factorial experimental design (FFED) was applied (where, k is the number of factors). It is a combination of mathematical and statistical technique to evaluate the relative significance of numerous effecting factors even in the existence of complex interactions (Myers and Montogomery 2001; Annadurai et al. 2003; Alkan et al. 2008). FFED determines which of the factors varies with the level of other factors. This experimental design is most widely used to determine main as well as interaction effects in which each variable is investigated at two levels i.e., low (-) and high (+) levels (Ricou-Hoeffer et al. 2001, Carmona et al. 2005).

Previously, Fractional Factorial Design experiment is used to study effects of various factors during the extraction of chromium using green emulsion liquid membrane in vegetable oil-based organic solvents (Noah et al. 2018). Biosorption of chromium using factorial design onto *Sargassum Sp*. was also studied (Carmona et al. 2005).

Although *S. glauca* is a more renewable, environmentally friendly, and cost-effective option, there hasn't been any research on using full factorial design to evaluate the impact of various controllable parameters on the effectiveness of chromium adsorption from aqueous medium on it. The optimal conditions for Cr(VI) adsorption by *S. glauca* have been evaluated using a 2^5 full factorial design experiment (FFED).

The steps in FFED involve designing of the experiments, regression analysis through ANOVA and F-test. This study offers an assessment of multiple factors and their interdependence. This experimental setup yields a lot of data, and also cuts down the number of runs, duration, and overall study expense. The impacts of individual parameters and their relative importance are derived, and the interaction of two or more elements can be determined, which are the most significant benefits of this technique (Lima et al. 2011). This study's application of a factorial design at two levels is one of its objectives in order to ascertain the impact of different parameters and their interactions on the efficacy of removing Cr (VI).

In real-world industries, column mode is preferred over batch study. Column treatment, also known as fixed bed or continuous pack bed, is a common adsorption technique in which the adsorbate solution is continually fed through a column having an adsorbent at a specific flow rate. Additionally, the adsorbent is continuously in touch with the adsorbate. The removal of larger amounts of wastewater with higher pollutant loads is commonly accomplished with this method. There are two different types of column adsorption. One is downstream treatment, where the solution of the adsorbate is passed in the same direction as gravity and another is upstream treatment, the same is transmitted in the reverse direction of gravity. The ability to absorb more adsorbate and the possibility for industrial use are benefits of this method (Patel 2021). *Strychnos mux vomica*, *Artocarpus heterophyllus*, *Ocimum basilium*, *Rhizopus arrhizus*, *Quercus crassipes*, *Aspergillus niger* etc. are some adsorbent previously reported to successfully adsorb Cr(VI) in fixed bed column (Nakkeeran et al. 2018; Saranya et al. 2018; Melo and D'Souza 2004, Yesim et al. 1999; Arnada- Garcia 2020, Mungasavalli et al. 2007).

The factorial design at two levels is implemented in order to ascertain the impact of different parameters and their interactions on the efficacy of removing Cr(VI). Further, the article includes the potential of *S. glauca* for the adsorption of Cr(VI) in the continuous flow method. Variation in parameters such as bed depth, flow rate and initial metal concentration was checked. The adsorption capacity was calculated using adsorption isotherm models. The present study deals with the scope of using *S. glauca in* continuously column mode to treat the Cr(VI) contaminated water.

Materials And Methods

Collection and Preparation of Biosorbent Material

S. glauca was used for biosorptive removal of Cr(VI) in the continuous mode from an aqueous solution. The plant was crushed, powdered, and sieved using the standard test sieve of 90 micron.

Preparation Of Stock And Standard Solutions

Analytical grade potassium dichromate was used for the preparation of chromium stock solution. All the solutions were prepared by using de-ionize or double distilled water. The pH of the solution was maintained using 0.1 N HCl and NaOH. All other working solution was prepared from the chromium stock solutions.

Method Of Analysis For Ffed

FFED determines which of the factors varies with the level of other factors. The number of runs at two levels is 2^k, where k is the number of factors. For the FFED 5 factors were considered (k = 5) each with low and high levels. Adsorbent (*S. glauca*) dose, pH, initial Cr(VI) concentration, temperature, and time were the five factors that were considered for the adsorption of hexavalent chromium from aqueous solution using *S. glauca*. The low (-) and the high (+) levels of each factor have been depicted in a Table 1 which was decided according to the preliminary experiments.

Table 1
Coded factors and their experimental levels.

Factors	Variables	Coded Symbol	Low level(-)	High level (+)
S. glauca Dose (g/L)	X_1	A	1	5
Initial Cr(VI) concentration (mg/L)	X_2	B	2	7
pH	X_3	C	10	100
Temperature(˚C)	X_4	D	15	40
Time (Min)	X_5	E	14	45

A matrix was created according to the factor’s levels using Minitab 19 software. The total number of experimental runs at two levels for each factor was 32 with 4 replicates. To avoid systematic error the experiments were performed in a randomized order. The response was the percentage removal of Cr(VI). The outputs of the experiments were examined using Minitab 19 software and the main and interaction effects were identified.

Method Of Analysis In Continuous Mode Adsorption

Well known fact is that the adsorption capacity of the biosorbent gets enhanced in the column mode in compare to the batch mode. Hence, *S. glauca* was used as a biosorbent in the continuous flow method to investigate the adsorption of hexavalent chromium. The experiment was performed in a column of diameter and height of 5 and 70 cm, respectively. Biosorbent was filled in the column with the support of glass beads on both sides. The analysis was done by varying the height of biosorbent (30, 35, 40 and 45 cm), initial chromium concentration (50, 100 and 150 mg/L) and flow rate (13 and 21 ml/min). The solution was pumped through the column using peristaltic pump. The outlet was collected every single hour and analysed for the residual hexavalent chromium and was continued till saturation point of the biosorbent.

Total fixed-bed capacity (q_{total}) was calculated using the formula

$$q_{total} = \frac{QA}{1000} = \frac{Q}{1000}\int_{t=0}^{t=t_{total}}(C_0 - C_t)d_t$$

where, Q is the flow rate (mL/min), A is the area under the breakthrough curve, t is the time of flow of solution, C_0 and C_t are the initial concentration of Cr(VI) in the aqueous solution and concentration of Cr(VI) ions at time t (min).

Further, by dividing the total fixed bed capacity with the biosorbent mass gives the uptake capacity of the column,

$$q_{exp} = \frac{q_{total}}{M}$$

Analysis Of The Hexavalent Chromium

After adsorption, residual Cr(VI) was analysed after each experimental run in both FFED and in continuous mode. The solutions were filtered using Whatman filter paper No. 42 and then the filtrates were analysed for residual Cr(VI). Insitu Cr(VI) was analysed using AQUANAL-plus chromium testing kit (Merck, Germany, range 0.005–0.1 mg/L). Colorimetrically Cr(VI) was determined in the laboratory by ultraviolet-visible spectrophotometry following the USEPA 7196A method.

Dilution was done for the sample having high Cr(VI) concentration and the dilution factor was calculated as :

$$\textbf{Dilution factor (DF)} = \frac{v_f}{v_i}$$

Where, V_f and V_i are the final and initial volume. In this case, the analysis yielded the following results:

Result Of Analysis = measurement Value X Dilution Factor

Mathematical model for column adsorption mode

Various models like Thomas model, Yoon-nelson model, were studied to predict the breakthrough curve which can easily predict the performance of adsorption column (Table 2).

Table 2
Mathematical expressions for different fixed-bed adsorption models.

Model	Equation	Linear equation	Plot	Parameters analyzed	Reference
Thomas	$\frac{C_t}{C_o}=\frac{1}{1+\exp\left(\frac{K_{TH}}{Q}(q_o x - C_0 V_{eff})\right)}$	$\ln\left(\frac{C_o}{C_t}-1\right) = K_T\left(\frac{q_{exp}}{Q} - C_o t\right)$	$\ln\left(\frac{C_o}{C_t}-1\right)$ against t	K_{TH} (L/min/mg) q_0 (mg/g)	Patel 2021
Yoon-Nelson	T=[$\frac{N_0 z}{C_o v}$] − [$\frac{1}{C_o K_{AB}}$] $\ln\left(\frac{C_o}{C_t}-1\right)$	$\ln\frac{C_t}{C_o - C_t} = K_{YN}t - \tau K_{YN}$	$\ln\frac{C_t}{C_o - C_t}$ against t	K_{YN} (min^{-}) τ (min)	Patel 2021
Adams- Bohart	$\frac{C_t}{C_o}=\frac{1}{1+e^{K_{YN}(\tau-t)}}$	$\ln\frac{C_t}{C_o} = K_{AB}C_o$ t -$K_{AB}N_o\frac{z}{U_o}$	$\ln\frac{C_t}{C_o}$ against t	K_{AB} (L/mg/min) N_o (mg/L)	Patel 2021

Result And Discussion

With the help of a full factorial design, the current paper examines the important variables that have a substantial impact on the effectiveness of hexavalent chromium (Cr(VI)). The relatively inexpensive and efficient way to improve a process has become its major attractiveness. Adsorbent dose (g/L), initial Cr(VI) concentration (mg/L), pH, temperature (˚C) and time (min) are the five variables screened for their potential impact on chromium removal.

For this purpose, 2^k full-factorial experimental design (FFED) was applied. It is a combination of mathematical and statistical technique to evaluate the relative significance of numerous effecting factors even in the existence of complex interactions (Myers and Montogomery 2001; Annadurai et al. 2003; Alkan et al. 2008). The steps in FFED involve designing of the experiments, regression analysis through ANOVA and F-test. FFED application was found efficient and also to obtain better response (Lima et al. 201; Ricou- Hoeffer et al. 2001, Carmona et al. 2005).

A 2^5 FFED (five factors each at two levels) was employed to evaluate the importance and interactions of the dose, pH, Cr(VI) concentration, temperature, and time for the adsorption of Cr(VI) onto *S. glauca*. The low (-) and the high (+) levels of each factor have been depicted in Table 1.

A matrix depicted in Table 3 was created according to the factor’s levels by Minitab 19 software. The total number of experimental runs at two levels for each factor was 32 with 4 replicates. To avoid systematic error the experiments were performed in a randomized order. The adsorption efficiency of Cr(VI) ions was the response variable in the study.

Table 3

2^5 Full-factorial design matrix for hexavalent chromium removal by *S. glauca*

No. of Runs	A	X_1	B	X_2	C	X_3	D	X_4	E	X_5	% Cr(VI) removal
1	1	-1	10	-1	2	-1	15	-1	15	-1	64
2	5	1	10	-1	2	-1	15	-1	15	-1	72
3	1	-1	100	1	2	-1	15	-1	15	-1	28
4	5	1	100	1	2	-1	15	-1	15	-1	31.54
5	1	-1	10	-1	7	1	15	-1	15	-1	18
6	5	1	10	-1	7	1	15	-1	15	-1	24.12
7	1	-1	100	1	7	1	15	-1	15	-1	12.47
8	5	1	100	1	7	1	15	-1	15	-1	16.45
9	1	-1	10	-1	2	-1	40	1	15	-1	89.15
10	5	1	10	-1	2	-1	40	1	15	-1	94.25
11	1	-1	100	1	2	-1	40	1	15	-1	54.25
12	5	-1	100	1	2	-1	40	1	15	-1	67.15
13	1	1	10	-1	7	1	40	1	15	-1	32.14
14	5	-1	10	-1	7	1	40	1	15	-1	44.15
15	1	1	100	1	7	1	40	1	15	-1	18.56
16	5	-1	100	1	7	1	40	1	15	-1	24.78
17	1	-1	10	-1	2	-1	15	-1	45	1	75.25
18	5	1	10	-1	2	-1	15	-1	45	1	82.56
19	1	-1	100	1	2	-1	15	-1	45	1	30.14
20	5	1	100	1	2	-1	15	-1	45	1	33.45
21	1	-1	10	-1	7	1	15	-1	45	1	21.56
22	5	-1	10	-1	7	1	15	-1	45	1	29.45
23	1	1	100	1	7	1	15	-1	45	1	19.54
24	5	-1	100	1	7	1	15	-1	45	1	26.56
25	1	1	10	-1	2	-1	40	1	45	1	95.85
26	5	-1	10	-1	2	-1	40	1	45	1	99.85
27	1	-1	100	1	2	-1	40	1	45	1	35.56
28	5	1	100	1	2	-1	40	1	45	1	46.54
29	1	-1	10	-1	7	1	40	1	45	1	45.56
30	5	1	10	-1	7	1	40	1	45	1	56.21
31	1	-1	100	1	7	1	40	1	45	1	27.45
32	5	1	100	1	7	1	40	1	45	1	36.56

The effect of the factor is defined as the change in response produced by a change in factor level and it was evaluated using factorial plots: main effects and normal probability plot. ANOVA and P values for adsorption of Cr(VI) were employed to ensure a good model. The results are displayed in Tables 4 and 5. Tables show main and interaction effects, coefficient of the model, R^2 (predicted)(adjusted), and probability for 2^5 FFED. The significance of the regression coefficient was determined by applying a student's t-test with a significance level of 5%.

Test Of Significance -anova

The ANOVA shows degree of freedom (DF) and sum of squares (SS) which are being used to estimate the factors effect and the F-ratios, which are defined as the ratio of respective mean-square-effect (MS) to the mean-square-error (MSE) and the probability value is used to verify whether a factor is significant. The significance of these effects was evaluated using the t-test, and had a significance level of 5% i.e., with a confidence level of 95%. The *R*-squared statistic indicated that the first-order model explained 99.97% of R's variability to the rejection of null hypothesis with a standard deviation of 0.47. Also, by definition the smallest level of $P < 0.05$ leads to the rejection of the null hypothesis (Table 4). Hence, The result revealed that main effect of each studied factors dose, pH, initial Cr(VI) concentration, temperature and time, and their 2-way (AC, AD, BC, BD, BE, CD, CE, DE), 3-way (ABC, ABD, ABE, ACE, BCD, BCE, BDE, CDE), 4-way (ABCD, BCDE) and 5-way interaction (ABCDE*)* are statistically significant (Table 4).

Table 4
Standard error coefficients, T- test and significance of adsorption of hexavalent chromium on *S. glauca.*

Term	Effect	Coef.	SE Coef.	T-Value	P-Value	Remark
A	7.2372	3.6186	0.0593	61.01	0.000	Significant
B	-27.4066	-13.7033	0.0593	-231.04	0.000	Significant
C	-34.1741	-17.0870	0.0593	-288.09	0.000	Significant
D	17.5422	8.7711	0.0593	147.88	0.000	Significant
E	4.4816	2.2408	0.0593	37.78	0.000	Significant
AB	-0.1941	-0.0970	0.0593	-1.64	0.112	Not Significant
AC	0.3734	0.1867	0.0593	3.15	0.004	Significant
AD	1.5747	0.7873	0.0593	13.27	0.000	Significant
AE	0.1753	0.0877	0.0593	1.48	0.150	Not Significant
BC	16.2559	8.1280	0.0593	137.04	0.000	Significant
BD	-3.6228	-1.8114	0.0593	-30.54	0.000	Significant
BE	-4.2897	-2.1448	0.0593	-36.16	0.000	Significant
CD	-3.1703	-1.5852	0.0593	-26.73	0.000	Significant
CE	4.6903	2.3452	0.0593	39.54	0.000	Significant
DE	-2.1472	-1.0736	0.0593	-18.10	0.000	Significant
ABC	-1.0353	-0.5177	0.0593	-8.73	0.000	Significant
ABD	1.2034	0.6017	0.0593	10.14	0.000	Significant
ABE	0.3278	0.1639	0.0593	2.76	0.010	Significant
ACD	0.0534	0.0267	0.0593	0.45	0.656	Not Significant
ACE	0.6803	0.3402	0.0593	5.74	0.000	Significant
ADE	-0.1722	-0.0861	0.0593	-1.45	0.157	Not Significant
BCD	-3.0528	-1.5264	0.0593	-25.74	0.000	Significant
BCE	4.4041	2.2020	0.0593	37.13	0.000	Significant
BDE	-2.6859	-1.3430	0.0593	-22.64	0.000	Significant
CDE	4.6316	2.3158	0.0593	39.04	0.000	Significant
ABCD	-1.8253	-0.9127	0.0593	-15.39	0.000	Significant
ABCE	0.1728	0.0864	0.0593	1.46	0.155	Not Significant
ABDE	0.2303	0.1152	0.0593	1.94	0.061	Not Significant
ACDE	-0.0072	-0.0036	0.0593	-0.06	0.952	Not Significant
BCDE	1.2678	0.6339	0.0593	10.69	0.000	Significant
ABCDE	0.4153	0.2077	0.0593	3.50	0.001	Significant

Table 5
Analysis of Variance for 2^5 design

Source	DF	Sum of squares	Mean of squares	F ratio	P value
Linear	5	36786.8	7357.4	32678.20	0.000
A	1	838.0	838.0	3722.16	0.000
B	1	12017.9	12017.9	53378.34	0.000
C	1	18685.9	18685.9	82994.46	0.000
D	1	4923.7	4923.7	21868.72	0.000
E	1	321.4	321.4	1427.30	0.000
2-Way Interactions	10	5362.1	536.2	2381.60	0.000
AB	1	0.6	0.6	2.68	0.112
AC	1	2.2	2.2	9.91	0.004
AD	1	39.7	39.7	176.22	0.000
AE	1	0.5	0.5	2.18	0.150
BC	1	4228.1	4228.1	18779.32	0.000
BD	1	210.0	210.0	932.71	0.000
BE	1	294.4	294.4	1307.70	0.000
CD	1	160.8	160.8	714.27	0.000
CE	1	352.0	352.0	1563.36	0.000
DE	1	73.8	73.8	327.64	0.000
3-Way Interactions	10	968.1	96.8	429.97	0.000
ABC	1	17.1	17.1	76.17	0.000
ABD	1	23.2	23.2	102.92	0.000
ABE	1	1.7	1.7	7.64	0.010
ACD	1	0.0	0.0	0.20	0.656
ACE	1	7.4	7.4	32.89	0.000
ADE	1	0.5	0.5	2.11	0.157
BCD	1	149.1	149.1	662.30	0.000
BCE	1	310.3	310.3	1378.36	0.000
BDE	1	115.4	115.4	512.68	0.000
CDE	1	343.2	343.2	1524.44	0.000
4-Way Interactions	5	80.4	16.1	71.38	0.000
ABCD	1	53.3	53.3	236.77	0.000
ABCE	1	0.5	0.5	2.12	0.155
ABDE	1	0.8	0.8	3.77	0.061
ACDE	1	0.0	0.0	0.00	0.952
BCDE	1	25.7	25.7	114.23	0.000
5-Way Interactions	1	2.8	2.8	12.26	0.001
ABCDE	1	2.8	2.8	12.26	0.001
Error	13	7.0	0.2		
Total	63	43208.2			

Regression equation of Cr(VI) uptake by S .glauca:

In this way the Cr(VI) uptake by *S. glauca* could be expressed using the following mathematical regression equation:

$\% Cr(VI) = b_0 + b_1X_1 + b_2 X_2 + b_3 X_3 + b_4 X_4 + b_5 X_5 + b_{12} X_1 X_2 + b_{13} X_1 X_3 + b_{14} X_1 X_4 + b_{15} X_1 X_5 + b_{23} X_2 X_3 + b_{24} X_2 X_4 + b_{25} X_2 X_5 + b_{34} X_3 X_4 + b_{35} X_3 X_5 + b_{45} X_4 X_5 + b_{123} X_1 X_2 X_3 + b_{124} X_1 X_2 X_4 + b_{125} X_1 X_2 X_5 + b_{134} X_1 X_3 X_4 + b_{135} X_1 X_3 X_5 + b_{145} X_1 X_4 X_5 + b_{234} X_2 X_3 X_4 + b_{235} X_2 X_3 X_5 + b_{245} X_2 X_4 X_5 + b_{345} X_3 X_4 X_5 + b_{1234} X_1 X_2 X_3 X_4 + b_{1235} X_1 X_2 X_3 X_5 + b_{1245} X_1 X_2 X_4 X_5 + b_{1345} X_1 X_3 X_4 X_5 + b_{2345} X_2 X_3 X_4 X_5 + b_{12345} X_1 X_2 X_3 X_4 X_5$

Where b_0 represents the global mean, b_i represents the estimation of the principal effect of the factors *i* for the response % Cr(VI), and $b_{ij,}$ b_{ijk} , b_{ijkl} and b_{ijklm} represents the estimation of the interaction effects between the factors *i, j, k, l*, and *m*. X_1, X_2, X_3, X_4, and X_5 are the dimensionless coded factors for A, B, C, D and E parameters. The mathematical model using Minitab 19 software is given by:

$\% Cr(VI) = 54.02 + 4.391 X_1 - 0.4715 X_2 - 6.089 X_3 + 1.4886 X_4 + 0.7948 X_5 - 0.05842 X_1 X_2 - 0.659 X_1 X_3 - 0.0991 X_1 X_4 - 0.0352 X_1 X_5 + 0.05800 X_2 X_3 + 0.003132 X_2 X_4 - 0.002237 X_2 X_5 - 0.1692 X_3 X_4 - 0.1317 X_3 X_5 - 0.01366 X_4 X_5 + 0.00992 X_1 X_2 X_3 + 0.002455 X_1 X_2 X_4 + 0.000428 X_1 X_2 X_5 + 0.02651 X_1 X_3 X_4 + 0.01068 X_1 X_3 X_5 + 0.000631 X_1 X_4 X_5 - 0.000571 X_2 X_3 X_4 + 0.000808 X_2 X_3 X_5 - 0.000248 X_2 X_4 X_5 + 0.004111 X_3 X_4 X_5 - 0.000472 X_1 X_2 X_3 X_4 - 0.000110 X_1 X_2 X_3 X_5 - 0.000015 X_1 X_2 X_4 X_5 - 0.000275 X_1 X_3 X_4 X_5 + 0.000015 X_2 X_3 X_4 X_5 + 0.000005 X_1 X_2 X_3 X_4 X_5$

Pareto Chart

Absolute values of main and interaction factors are illustrated in Pareto Chart (Fig. 1) in the horizontal columns. The vertical line (near 0) indicates non-significance magnitude for effects for an α risk of 5%. According to the *F*-value, p-value (Table 4) and pareto chart (Fig. 1) it seems that interactions AB, AE, ACD, ADE, ABCE & ABDE are statistically not significant. Also, the main factors are found independent of each other.

Main Effect Plot For Cr(Vi) Adsorption

The main effect of each parameter on the Cr(VI) ion adsorption is shown in Fig. 2 which help to visualize which factors affects the adsorption (adsorption efficiency) the most. The more slope is near zero, the less will be its effect.

The effect of dose temperature and time are positive facilitating the adsorption since there is an increase in adsorption efficiency of Cr(VI) was found when these factors are changed from low to high level. Whereas the effect of initial concentration of Cr(VI) and pH are found to be negative as the percentage removal for Cr(VI) decreases when these factors are changed from low to high level.

Interaction Plot For Cr(Vi) Adsorption

The interaction plot was also studied (Fig. 3). In interaction plot the parallel line shows no significant interactions between the studied factors. However a significant interaction has been observed between initial Cr(VI) concentration and pH. This indicates that increasing the concentration from 10 to 100 mg/L decreases the adsorption at higher pH and the adsorption efficiency of *S. glauca* is higher at lower concentration and pH. Also increasing the concentration from 10 to 100 mg/L and time from 15 to 45 minutes significantly decreases the adsorption percentage. Adsorption efficiency also decreases when the pH and time is simultaneously changed from low to high level. This interaction remains non-significant. Most Significantly, the study shows that raising the *S. glauca* biosorbent dose effectively enhances the rate of Cr(VI) adsorption, suggesting that increasing the biosorbent dose will be effective in removing waste water with a high content of Cr(VI). The rise in elimination percentage due to increased biosorbent dose can be beneficial for column research.

Normal Probability Plot For Cr(Vi) Adsorption

The normal probability plot shown in Fig. 4 confirms the results given in Table 4. C, B, BE, BC, CD, DE, ABC, BCD, BDE and ABCD lie to the left of the line, their contribution had a negative effect. A, D, E, AC, AD, CE, BC, ABE, ACE, ABD, BCE, CDE, BCDE and ABCDE lie on the right side and show positive effect. The pH (C) had largest effect because it lies farthest from the zero line. Rest 7 points (AB, AE, ACD, ADE, ABCE, ABDE and ACDE) lying on the zero line has no significant effect on the adsorption of Cr(VI) on *S. glauca* (Fig. 4).

Operational Parameters Of Packed Bed Column

Packed bed adsorption column design and operation is essential for up-scaling the batch experiment. The efficiency of adsorption column is evaluated through break through curve. Essential parameter like flow rate, bed depth and initial metal ion concentration were studied through small scale adsorption column experiments which affect the time for appearance and shape of breakthrough curve. The shape of breakthrough curve is obtained by plotting the amount of Cr(VI) adsorbed (C_t/C_0) as a function of time in adsorption column. Where C_t is the Cr(VI) concentration in effluent and C_0 is the Cr(VI) concentration in influent. Breakthrough point in the experiment is considered to occur when $C_t/C_0 = 0.05$ which is the permissible limit of Cr(VI) in drinking water (Yahya et al. 2020). The exhaustion point of the break through curve is assumed when $C_t/C_0 = 0.95$.

Initial Metal Ion Concentration

Adsorption column efficiency was investigated at different Cr(VI) ion concentration of 50 mg/l, 100 mg/l and 150 mg/l at constant flow rate of 13 ml/min and bed depth of 35 cm. Figure 5 concludes with the increase in initial concentration of Cr(VI) in the influent, the breakthrough curve becomes steeper. However, in all concentration of metal ion the breakthrough curve is S shaped. Experimental results shown in Table 6 reveals that on increasing the initial Cr(VI) concentration, the breakthrough point and exhaustion point is achieved at shorter time. The Cr(VI) uptake (q_{exp}) at breakthrough point increased from 220 to 287 mg/g and at exhaustion point it increased from 333 to 545.2 mg/g. This phenomenon may be due to increased loading of initial metal ion concentration to the adsorption column which rapidly uses the binding sites of adsorbent for surface adsorption indicating that the diffusion process in concentration dependent (Hussain et al. 2022). Lower initial metal ion concentration depicted comparatively longer breakthrough point and exhaustion point. Further greater volume of influent could be treated due to longer contact time between metal ion and adsorbent. This may be due to decreased driving force caused by lower Cr(VI) concentration resulting in overall decrease in the diffusion of Cr(VI) onto *S. glauca*. The result is in accordance with the removal of Cr(VI) as reported in literature (Albadarin et al. 2012). However, the adsorption capacity (q_{exp}) of the adsorbent increases on increasing the metal ion concentration. This may be due to increased binding sites due to increased surface area and pores in *S. glauca* (Luo et al. 2011). Though the adsorption capacity is higher in case of high initial concentration of Cr(VI), the lower concentration of Cr(VI) desirable in operating condition in order to get larger volume of influent treated till the breakthrough point is achieved.

Effect Of Bed Depth On Breakthrough Curves

Adsorption column performance at different bed depth (30 cm, 35 cm, 40 cm, 45 cm) with a constant Cr(VI) concentration of 100 mg/L and flow rate of 13 mL/min are shown in Fig. 6. The break through curve becomes less steep on increasing the bed height. However the increased bed depth resulted in higher removal of Cr(VI) by *S. glauca* with increased breakthrough time (t_b) and exhaustion time (t_e) thereby improving the adsorption efficiency of adsorbent Table 6. The Cr(VI) uptake (q_{exp}) at breakthrough point increased from 244.8 to 381.8 mg/g and at exhaustion point increased from 454.5 to 611.7 mg/g when the bed height was increased from 30 to 45 cm respectively. Reason cited for this phenomena included the higher bed heights resulted in increased adsorption site for binding Cr(VI) on the surface of *S. glauca* as seen in Table 6 (Kumar and Chakraborty 2009). In low bed height Cr(VI) spends less time for diffusion onto the surface of *S. glauca* (Omitola et al. 2022).

Effect Of Flow Rate

The effect of different flow rates (13 and 21 ml/min) on the performance of adsorption column was studied at constant adsorbent dose of 76 g and initial Cr(VI) ions concentration of 100 mg/l at pH 2.5 (Fig. 7). Cr(VI) removal efficiency by *S. glauca* in adsorption column decreases with increase in flow rate. The adsorption capacity at exhaustion point decreases from 520 mg/l to 110.8 mg/l for flow rate 13 and 21 ml/min respectively (Table 6). Similar results were obtained by researchers indicating slower diffusion of Cr(VI) on to *S. glauca* at higher flow rate due to decreased residence time of Cr(VI) ions in the adsorbent column This causes early appearance of breakthrough point and exhaustion point and lower adsorption (Kumar and Chakraborty 2009, Rangabhashiyam et al. 2016).

Table 6
Adsorption capacity of hexavalent chromium onto *S. glauca* in a fixed-bed column by varying different parameters

Initial Concentration C_o (mg/L)	pH	Flow rate Q (mL/min)	Bed Depth Z (cm)	Effluent volume at t_b (L) (C_t/C_o= 0.05)	q_{exp} at t_b (mg/g)	Effluent volume at t_e (L) (C_t/C_o= 0.95)	q_{exp} at t_e (mg/g)
100	2.5	13	30	29.54	244.82	29.54	454
100	2.5	13	36	33.86	329.41	33.86	518.23
100	2.5	13	40	37.58	330.7	37.58	566.40
100	2.5	13	45	39.98	381.87	39.98	611.69
100	2.5	13	36	32.76	329.41	32.76	519.91
100	2.5	21	36	18.05	58.15	18.05	110.8
50	2.5	13	36	36.96	220.5	36.96	333
100	2.5	13	36	32.76	349.41	32.76	518.23
150	2.5	13	36	27.72	287.15	27.72	545.26

Thomas Model:

Thomas model for continuous study helps to evaluate the adsorption rate constant and solid phase concentration of the hexavalent chromium on *S. glauca*. It is most widely used model for the evaluation of concentration–time breakthrough curve in column studies. The Thomas adsorption model helps to determine the maximum solid-phase concentration of adsorbate on adsorbent and its rate constant. This model is based on the assumptions of Langmuir kinetics of adsorption and desorption. Thomas model shows that the rate driving forces follows second-order and reversible kinetic reaction. This also shows no axial dispersion. Thomas model's parameters can be calculated by the linearized equation.

$$\mathrm{Ln}\ [C_oC_t\text{-}1] = K_T\ q_oQ\text{-}\ C_ot$$

Where, K_T (mL/min mg) is the Thomas model constant, q_o (mg/g) is the adsorption capacity, m is amount of adsorbent in the column (g), and t is the total flow time (min).

The model parameter K_T and q_o is calculated by slope and intercept respectively through a linear plot of $\ln[(C_o/C_t) - 1]$ versus t (Fig. 8).

The value of K_T was found to decrease with increase in initial concentration and bed height whereas it increased with increase in flow rate. The adsorption capacity increased with increase in initial concentration and bed height and decreased with increase in flow rate. Similar study was observed by Hana et al. (2009) and Sobhy et al. (2019). The R^2 value from Thomas model was found to be 0.99 in all studied parameters except for the flow rate of 21 ml/min. Also the value of q_o for all studied parameters is found very close to the experimental results (Table 7). In this respect, Thomas model is applicable for describing the adsorption of Cr(V)) onto *S. glauca* (Ahmad and Hameed 2010). According to Thomas model, the adsorption equilibrium predicts monolayer (Langmuir adsorption) and obeys second order reversible kinetics adsorption. This has been verified by our earlier batch adsorption studies where Langmuir model corresponds best (Banchhor et al. 2020).

Yoon–nelson Model

The Yoon–Nelson is relatively simple model for single component system. The model is based on the assumption that the rate of decrease in the probability of adsorption for each adsorbate molecule is proportional to the probability of adsorbate adsorption and the probability of adsorbate breakthrough on the adsorbent (Yoon and Nelson 2010). The linearised form of model is expressed in Table 2. Yoon-Nelson plot between $\ln(C_t/(C_o - C_t))$ verses t was generated to obtain a complete breakthrough curve to check adsorption column efficiency (Fig. 8). The slope of S shaped curve will give the value of K_{YN} and the intercept gives the value τ at different concentrations, bed height, and flow rates presented in Table 7. As expected τ decreases with the increase in initial concentration of (Cr(VI) with the increase in K_{YN}, this may be due to exhaustion of available binding sites in *S. glauca* for 50% breakthrough (Shrivastava et al. 2018). Similar results were obtained for increasing flow rate, τ decreases and K_{YN} increases may be due to less retention time of Cr(VI) on *S. glauca* (Shrivastava et al. 2018). On increasing the bed height, τ increases with the decrease in K_{YN} may be due to availability of more binding sites in the *S. glauca*. Ajmani et al. got similar trend in adsorption of Cr(VI) column study (Ahmad et al. 2012). Further it is observed that the correlation coefficients (R^2) were found to be 0.99 which shows better fit of the model along with the Thomas model.

Adams-bohart Model:

The model assumes that the rate of reaction is proportional to the residual capacity of the adsorbent or to the concentration of the adsorbate. The values K_{AB} and N_o were calculated from the slope and intercept of the plot $\ln(C_t/C_o)$ vs t using the linearised form of the equation (Table 2) (Fig. 8). The correlation coefficients obtained for the flow rate breakthrough curves were found to range from 0.94 to 0.99 suggesting that initial process of the system can be predicted through this model (Table 7). The values of K_{AB} and N_o obtained for bed heights started to decrease with the increase in bed height. In the case of initial metal ion concentration, N_o increases with the increase in initial metal ion concentration while values of K_{AB} decreases. For the flow rate the values of K_{AB} and N_o increases with the increase in flow rate. These observations suggest that the Adams–Bohart model is not as applicable to the present system of adsorption as compare to Thomas and Yoon-Nelson models.

The adsorption capacity obtained in column mode is 333 mg/g, 518 mg/g and 545.2 mg/g for initial metal ion concentration of 50mg/l, 100mg/l and 150 mg/l respectively. The value is extremely higher than our previous batch mode study which is 10 mg/g (Banchhor et al. 2020). The reason may be due to enhanced residence time between adsorbate and adsorbent. Also due to increased surface area and pores in adsorbent in column study with reference to the reported literature.

Table 7
Parameters of Thomas, Yoon-Nelson and Adams-Bohart Models.

Initial Concentration C_o (mg/L)	Flow rate Q (mL/min)	Bed Depth Z (cm)	Volume used (L)	Thomas Model				Yoon- Nelson Model				Adams-Bohart Model			
				$K_T * 10^{-3}$ (L/min mg)	q_o (mg/g)	q_{exp} (mg/g)	R^2	K_{YN}	τ (hrs)	τ(exp) (hrs)	R^2	U_0 Linear Velocity	K_{AB} x 10^{-3}	N_o	R
100	13	30	29.54	3.74	501.72	454	0.99	0.374	27	28	0.99	0.81	2.58	90.82	0
100	13	36	33.86	3.53	523.30	518.23	0.99	0.352	31	32	0.99	0.81	2.39	87.79	0
100	13	40	37.58	3.14	532.03	566.40	0.99	0.314	35	36	0.99	0.81	2.22	86.65	0
100	13	45	39.98	2.97	547.86	611.69	0.99	0.301	39	40	0.99	0.81	2.14	83.75	0
100	13	36	32.76	3.5	522.30	519.91	0.99	0.356	31	32	0.99	0.81	2.41	87.45	0
100	21	36	18.05	7.7	308.61	110.8	0.98	0.43	26.3	27	0.99	1.32	3.22	119.45	0
50	13	36	36.96	6.84	300.48	333	0.99	0.344	36	36	0.99	0.81	5.38	35.13	0
100	13	36	32.76	3.5	522.38	518.23	0.99	0.35	31.34	32	0.99	0.81	2.45	88.72	0
150	13	36	27.72	2.6	652.6	545.26	0.99	0.398	25	27	0.99	0.81	1.9	135.82	0

Conclusion

The selected adsorbent may be viewed as useful material while considering economic aspects of waste water treatment. The obtained results are summarized as follows:

Following conclusions can be drawn from the present study:

1. Utilizing a two-level complete factorial design, the response variable for the elimination of chromium was established, as well as the data was statistically validated. The results of this study indicate that full factorial design is capable to predict the significant factors affecting hexavalent chromium extraction by using *S. gluaca*. The elimination of chromium was found to be significantly influenced by all five parameters which were evaluated based on a normal probability plot of standardized effects, t-value and p-value, a Pareto chart, main effects and interaction plots at 5% significance level using the Minitab 19 software. Analysis of variance (ANOVA) and predicted chromium removal from the model at 95% confidence interval against the experimental result is used to examine the adequacy of the developed empirical relationship regression model. Most significantly the study helps to conclude that the *S. glauca* dose effectively enhances the rate of Cr(VI) adsorption from waste water, which is helpful in up-scaling the batch adsorption mode to the column adsorption mode.
2. Continuous mode is more preferable than batch study in practical industries. So the adsorption potential of *S. glauca* was checked using the column adsorption mode. The maximum adsorption capacity was found to be 611 mg/g when initial inlet concentration was 100 mg/L with a bed depth of 45 cm at ph 2.5 and the flow rate was maintained at 13 ml/min. It has been found during the study that for initial Cr(VI) concentration of 100 mg/L at bed depth of 45 cm maximum volume of water is treated whose concentration falls below the prescribed limit of 0.05 mg/L Cr(VI). Lower concentration of Cr(VI) desirable in operating condition in order to get larger volume of influent treated till the breakthrough point is achieved. The adsorption equilibrium was observed to follow monolayer adsorption and second order reversible kinetics as depicted by Thomas adsorption model.

Declarations

Competing Interests: The authors declare that they have no known competing financial interests or personal relationships that could have appeared to influence the work reported in this paper.

Funding: The research work has been carried out under the PhD program at Bhilai Institute of Technology, Durg.

Acknowledgement: We highly acknowledge Bhilai Institute of Technology, Durg, CG for providing th facilities to carry out the experiments.

References

1. Ahmad AA, Hameed BH (2010) Fixed-bed adsorption of reactive azo dye onto granular activated carbon prepared from waste. Journal of Hazardous Materials 175:298–303.
2. Ajmania A, Patra C, Subbiah, S, Narayanasamya S (2020) Packed bed column studies of hexavalent chromium adsorption by zinc chloride activated carbon synthesized from Phanera vahlii fruit biomass. Journal of Environmental Chemical Engineering 8:103825 https://doi.org/10.1016/j.jece.2020.103825
3. Albadarin AB, Mangwandi C, Al-Muhtaseb A, Ahmad MNM (2012) Modelling and Fixed Bed Column Adsorption of Cr(VI) onto Orthophosphoric Acid-activated Lignin. Chinese Journal of Chemical Engineering 20(3):469-477. DOI: 10.1016/S1004-9541(11)60208-5.
4. Alkan M, Kalay B, Dogan M, Demirbas O (2008) Removal of copper ions from aqueous solutions by kaolinite and batch design. Journal of Hazardous Materials 153(1-2): 867-876.
5. Annadurai G, Juang RS, Lee DJ (2003) Adsorption of heavy metals from water using banana and orange peels. Water Science and Technology 7(1):185-190.
6. Arnada-Garcia E, Cristiani-Urbina E (2020) Hexavalent chromium removal and total chromium biosorption from aqueous solution by *Quercus crassipes* acorn shell in a continuous up-flow fixed bed column: influencing parameters, kinetics, and mechanism. Plos one DOI 10.1371/journal.pone.0227953.
7. Bayuo J (2021) An extensive review on chromium(VI) removal using natural and agricultural wastes materials as alternative biosorbents. Journal of environmental health science and engineering 19(1):1193-1207 Doi: 10.1007/s40201-021-00641-w
8. Carmona MER, Da Silva MAP, Leite SGF (2005) Biosorption of chromium using factorial experimental design. Process Biochemistry 40:779-788.
9. Hana R, Wanga Y, Zhaoc X, Wanga Y, Xieb F, Chengb J, Tanga M (2009) Adsorption of methylene blue by phoenix tree leaf powder in a fixed-bed column: experiments and prediction of breakthrough curves. Desalination 245:284–297. DOI:10.1016/j.desal.200 .0 .08 7 13
10. Hasan SH, Ranjan D, Talat M (2010) Agro-industrial waste wheat bran for the biosorptive remediation of selenium through continuous up-flow fixed-bed column, Journal of Hazardous Materials 181:1134–1142.
11. Hussain D, Khan SA, Alharthi SS, Khan TA (2022) Insight into the performance of novel kaolinite-cellulose/cobalt oxide nanocomposite as green adsorbent for liquid phase abatement of heavy metal ions: Modelling and mechanism. Arabian journal of chemistry 15(7).
12. Lima LS, Araujo MDM, Quináia SP, Migliorine DW, Garcia JR (2011) Adsorption modelling of Cr, Cd, and U on activated carbon of different origins by using fractional factorial design. Chemical Engineering Journal 166:881–889. DOI: 10.1016/j.cej.2010.11.062
13. Luo X, Deng Z, Lin X, Zhang C (2011) Fixed-bed column study for Cu^{2+} removal from solution using expanding rice husk. Journal of Hazardous Materials 187(1–3):182-189.
14. Melo JS, D’Souza SF (2004) Removal of chromium by mucilaginous seeds of Ocimum Basilicum. Bioresource Technology 92(2):151-155.

15. Mungasavalli DP, Viraraghavan T, Jin Y (2007) Biosorption of chromium from aqueous solutions by pre-treated *Aspergillus niger*. Batch and column studies. Colloids and Surfaces 301:214-223.

16. Myers RH, Montgomery DC (2001) Response surface methodology Wiley, 2nd Edition.

17. Nakkeeran E, Patra C, Shahnaz T, Ragabhashiyam S, Selvaraju N (2018) Continuous biosorption assessment for the removal of hexavelnt chromium from aqueous solutions using Stychnos nux vomica fruit shell. Bioresource Technology Reports 3:256-260.

18. Noah NFM, Othman N, Jusoh N (2018) The use of factorial design in screening of factors influencing hexavalent chromium extraction by continuous green emulsion liquid membrane. Materials Science and Engineering DOI 10.1088/1757-899X/458/1/012032

19. Omitola OB, Abonyi MN, Akpomie KG (2022). Adams-Bohart, Yoon-Nelson, and Thomas modeling of the fix-bed continuous column adsorption of amoxicillin onto silver nanoparticle-maize leaf composite. Applied Water Science 12:94. https://doi.org/10.1007/s13201-022-01624-4

20. Patel H (2021). Comparison of batch and fixed bed column adsorption: a critical review. International Journal of Environmental Science and Technology DOI- 10.1007/s13762-021-03492-y.

21. Potsangbam AK, Chakraborty S (2009). Fixed-bed column study for hexavalent chromium removal and recovery by short-chain polyaniline synthesized on jute fiber. Journal of Hazardous Materials 162:1086–1098.

22. Rangabhashiyam S, Suganya E, Selvaraju N (2016) Packed bed column investigation on hexavalent chromium adsorption using activated carbon prepared from Swietenia Mahogani fruit shells. Desalination and Water Treatment 57(28).

23. Ricou-Hoeffer P, Lecuyer I, LeCloirec P (2001). Experimental design methodology applied to adsorption of metallic ions onto fly ash. Water Research 35(4):965–976.

24. Sag Y, Atacoglu I, Kutsal T (1999). Simultaneous biosorption of chromium (VI) and Copper(II) on *Rhizopus arrhizus* in packed column reactor: Application of the competitive Freundlich model. Separation Science and Technology 34(16):3155-3171.

25. Saranya N, Ajmani A, Sivasubramanian V, Selvaraju N (2018). Hexavalent chromium removal from simulated and real effluents using Artocarpus heterophyllus peel biosorbent – Batch and continuous studies. Journal of Molecular Liquids 265(1):779-790.

26. Sharma P, Singh SP, Parakh SK, Tong YW (2022) Health hazards of hexavalent chromium (Cr(VI)) and its microbial reduction. Bioengineered 13(3):4923-4938 DOI: 10.1080/21655979.2022.2037273

27. Sobhy M, Yakouta Hassanc R, Omarc HA (2019) Fixed-bed column study for the removal of hexavalent chromium ions from aqueous solutions via pyrolysis of rice husk. Desalination and Water Treatment 170:128–137.

28. Srivastava S, Agrawal SB, Mondal MK (2018). Fixed Bed Column Adsorption of Cr(VI) from Aqueous Solution Using Nanosorbents Derived from Magnetite Impregnated Phaseolus vulgaris. Environmental Progress & Sustainable Energy 38(1):568-576 DOI 10.1002/ep.12918

29. Yahya MD, Aliyu AS, Obayomi KS, Olugbenga AG, Abdullahi UB (2020) Column adsorption study for the removal of chromium and manganese ions from electroplating waste water using cashew nuts adsorbent. Cogent Engineering 7:1748470. Doi:10.1080/23311916.2020.1748470

30. Yoon YH, Nelson JH (2010) Application of Gas Adsorption Kinetics I- A Theoretical Model for Respirator Cartridge Service Life. American Industrial Hygiene Association Journal 45(8):509-516. DOI: 10.1080/15298668491400197

Figures

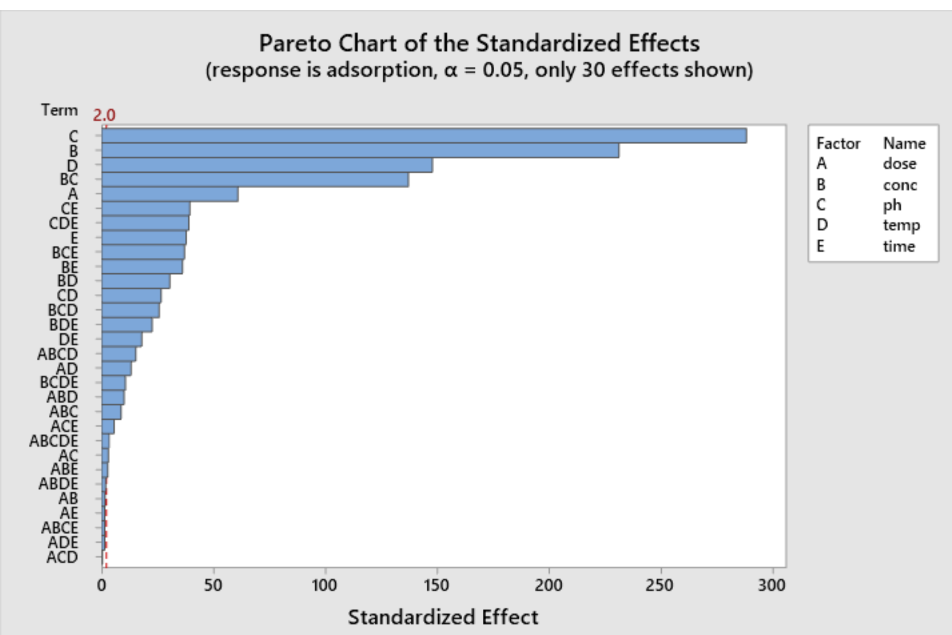

Figure 1

Pareto Chart

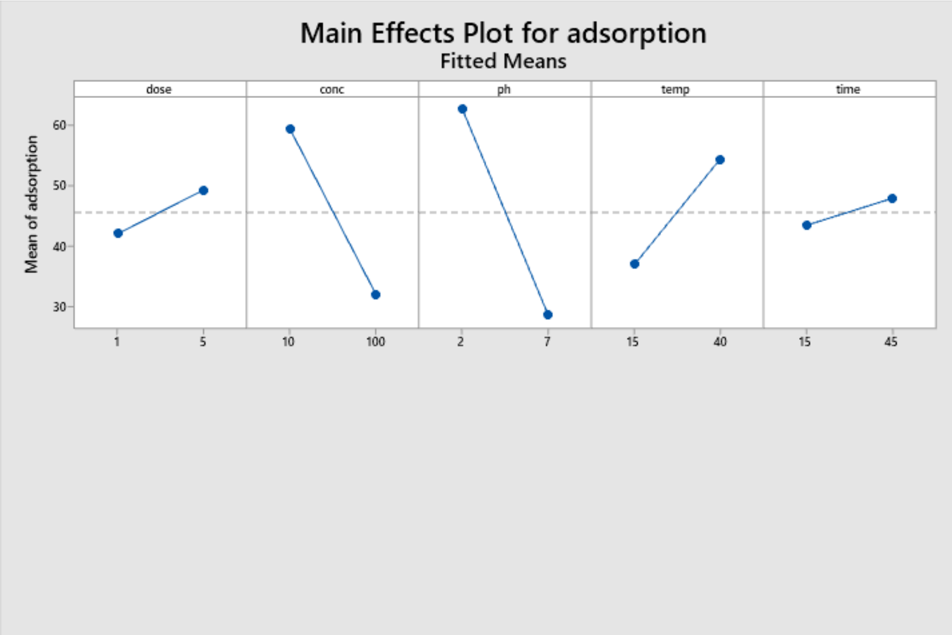

Figure 2

Main effect plot for adsorption

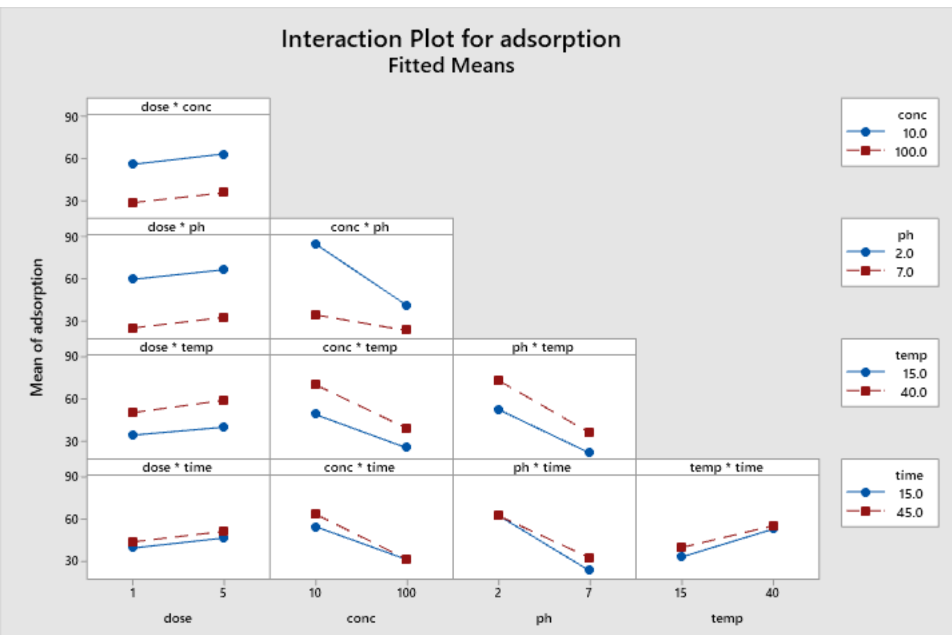

Figure 3

Interaction plot for all factors responsible for adsorption

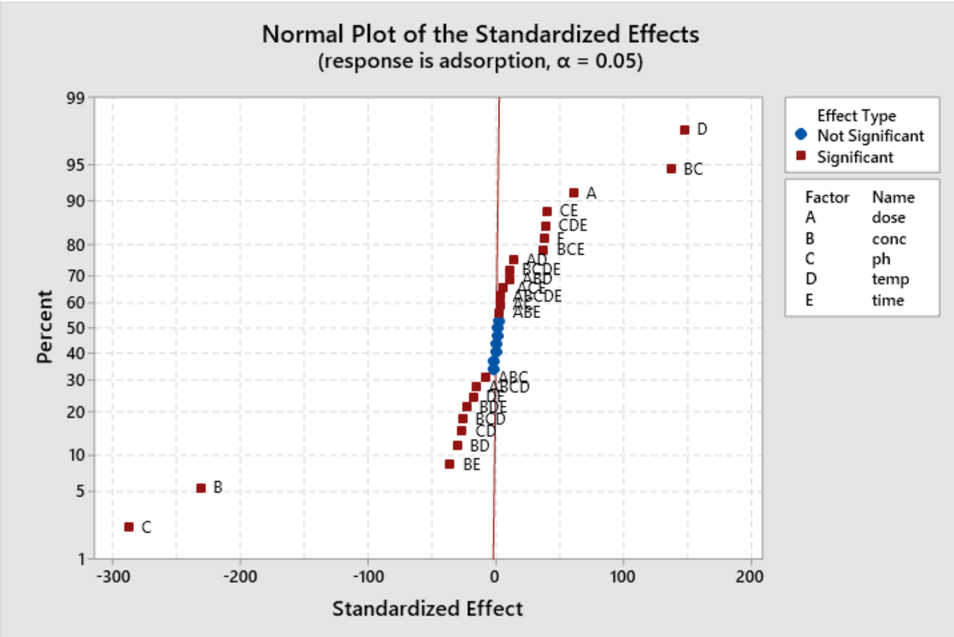

Figure 4

Normal plot of the standardized effects

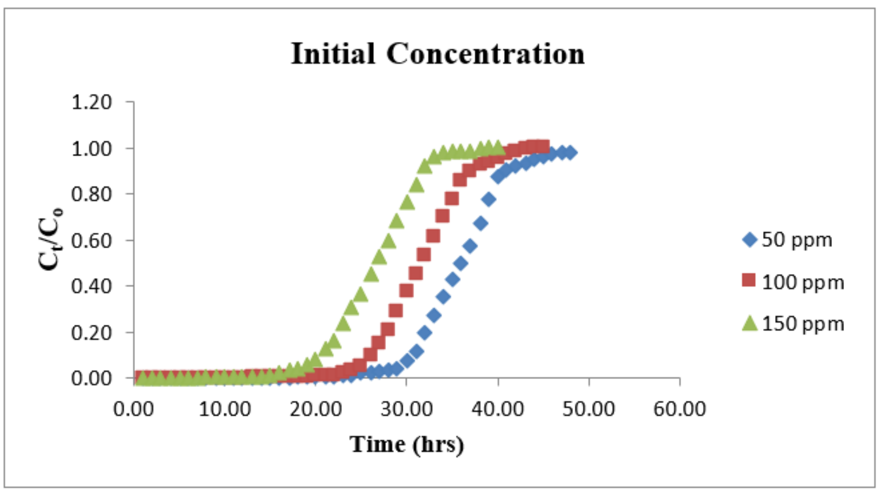

Figure 5

Breakthrough curve of metal ions at different concentration (50, 100,150 ppm)

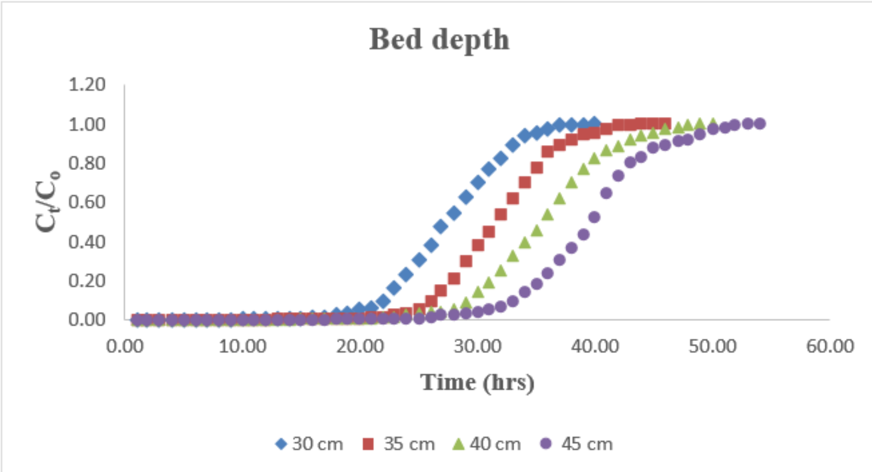

Figure 6

Breakthrough curve of Cr(VI) adsorption using different bed depth of adsorbent *S. glauca*

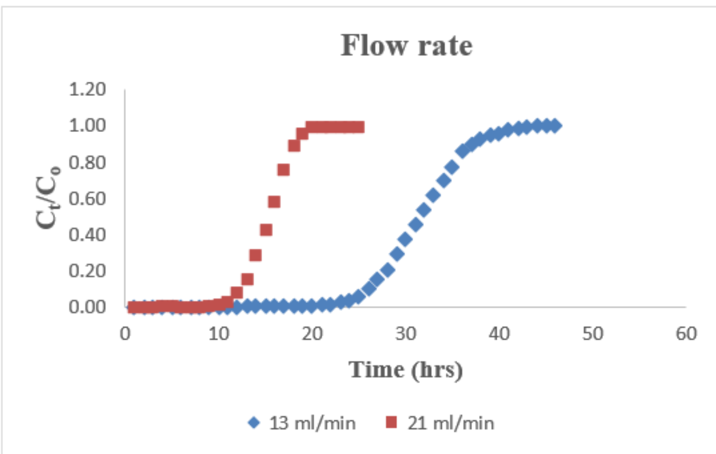

Figure 7

Breakthrough curve of Cr(VI) adsorption varying the flow rate of influent

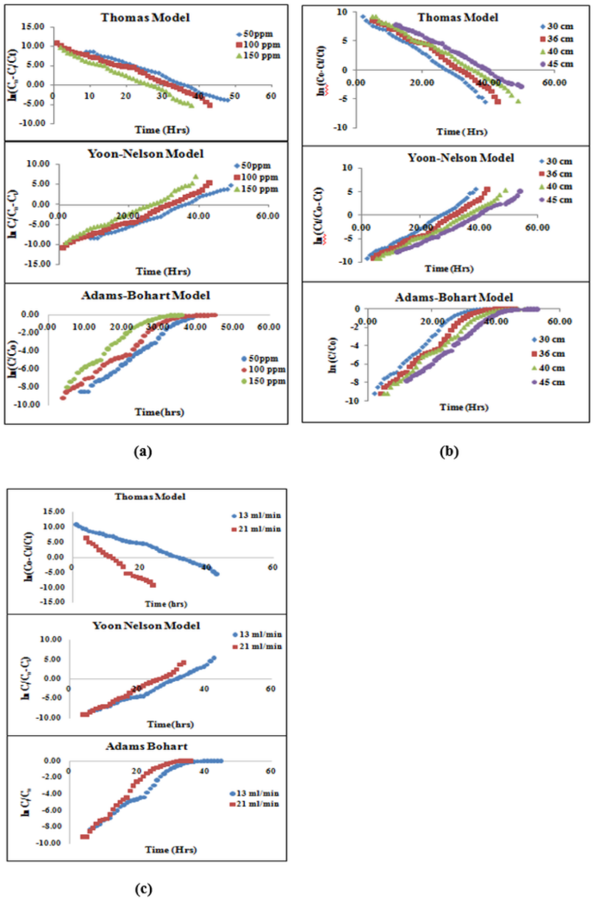

Figure 8

Fixed-bed adsorption models for parameters (a) initial Cr(VI) concentration, (b) bed depth, (c) flow rate